communications medicine

A Nature Portfolio journal

Matters arising

https://doi.org/10.1038/s43856-025-00880-0

The non-cytotoxic small molecule NPB does not inhibit BAD phosphorylation and forms colloidal aggregates

John Maringa Githaka[1,3], Tomás Gutiérrez[1,3], Zhuang Zhuang Han[1], Joseph O. Primeau[1], Heather Muranyi[1], Howard S. Young[1], Brian D. Sykes[1], Olivier Julien[1] ✉ & Ing Swie Goping[1,2] ✉

ARISING FROM X. Zhang et al. *Communications Medicine* https://doi.org/10.1038/s43856-022-00142-3 (2022)

Therapies that induce apoptosis in cancer cells are critically important in clinical oncology. In a recent Communications Medicine article[1] and Proceedings of the National Academy of Sciences article[2], a small molecule, NPB, was reported to induce cancer cell-specific cell death by inhibiting phosphorylation of the apoptotic protein, BAD. Using the same breast and ovarian cancer cell lines as the original reports, we endeavored to replicate these studies. We found that NPB did not inhibit BAD phosphorylation nor induce cell death. Furthermore, we observed that NPB forms large colloidal aggregates that are incompatible with the proposed mechanism of action, which posits that NPB binds to intracellular BAD. Thus, the prospect of NPB as a BAD-inhibitor that induces cancer cell apoptosis should be re-evaluated.

The BH3-only BCL-2-associated agonist of cell death protein BAD plays a key role in sensitizing cells to apoptosis[3,4]. This activity is regulated through coordinated phosphorylation of three key serine residues S75, 99 and 118[3,4]. Unphosphorylated BAD interacts with Bcl-XL, and triggers the apoptotic program by liberating pro-apoptotic BAX/BAK to initiate cell death[5,6]. Thus, inhibition of BAD phosphorylation is a rational approach to stimulate therapeutic cancer cell death. Pandey et al.[2] identified a small molecule termed NPB that interacted with BAD and inhibited its phosphorylation on S99. This group reported that NPB reduced cell viability in multiple cancer cells lines and was not toxic to non-transformed cells[1,2]. Given that our own investigations identified a role of BAD in breast cancer and mammary gland development[7–10], we wanted to incorporate this BAD-inhibitor into our studies.

We purchased NPB (Axon Medchem, cat# 3079) and confirmed its purity and structure. Mass spectrometry showed a relatively pure compound of expected target mass. ^{1}H nuclear magnetic resonance (NMR) spectroscopy profiles were similar to the published report[2] and we confirmed the chemical structure with 1D ^{1}H, 2D ^{1}H-^{1}H-COSY and ^{1}H,^{13}C HSQC correlation spectra (Fig. 1a. Sup Fig. 1). We then wanted to confirm that NPB inhibits BAD-S99 phosphorylation using the same breast cell lines, treatment conditions, and assay methods as originally reported[2]. Unexpectedly, we found NPB did not decrease the levels of BAD-Ser99 phosphorylation (Fig. 1b). Antibody specificity was validated with negative-control cell lysates wherein S75/99/118 residues of BAD are mutated to alanines[10] and positive control lysates wherein BAD-S99 phosphorylation was either stimulated with paclitaxel or inhibited with staurosporine or serum starvation (Sup Fig. 2)[11,12]. We next assessed the effect of NPB on cell viability (Fig. 1c, left panel; Supp. Fig. 3) with multiple time courses, using the methodologies published by the original group[1,2]. NPB treated cells (magenta) remained mostly viable, similar to DMSO-treated control cells (black line) and rarely reached maximal cell death defined by H_2O_2-treatment (dotted black line). Thus computed IC_{50} values would be inaccurate, but nevertheless would be far greater than the originating group's published values of 4.8 to 7.2 μM[2]. On the other hand, the apoptotic agent staurosporine induced robust cell death in the expected low micromolar ranges (Fig. 1c, right panel). The same originating group also published recently that NPB was cytotoxic to ovarian cancer cell lines[1]. We found NPB did not alter BAD phosphorylation or cell viability in a subset of the reported ovarian cancer cell lines (Fig. 1d, e). We contacted the originating group[2] and they provided us with their synthesized NPB. We performed high-resolution ^{1}H NMR and confirmed that the commercial and originating NPBs were nearly indistinguishable. (Supp. Fig. 4a). The originating NPB was tested on breast cancer cell lines and had the same lack-of-effect as the commercial source (Supp. Fig. 4b). The originating NPB also failed to decrease BAD phosphorylation (Supp. Fig. 4c). Thus, we could not replicate the reported inhibitory effect of NPB on BAD-phosphorylation, nor the reported cytotoxic effect in multiple cell lines, using both commercial NPB and the NPB synthesized by the original reporting group.

We did note apparent viability loss in two cell lines at the highest NPB concentration (Fig. 1c; BT549 and MCF10A; 100 μM), however, solution turbidity indicated that NPB was insoluble. Hydrophobic small molecules similar in structure to NPB are known to form insoluble colloidal aggregates in aqueous solutions. Indeed, the online tool "Aggregator Advisor"[13] labeled NPB as a suspicious aggregator. We used dynamic light scattering to determine the hydrodynamic size of NPB in serum-free RPMI. NPB showed concentration dependent increases in average particle size (Fig. 2a; 1 μM = 426.4 nm, 10 μM = 801.8 nm, 100 μM = 893.7 nm, see Supplementary Data file), with a critical aggregation concentration of approximately 0.1 μM (Fig. 2b). Similar results were obtained in water. Electron microscopy of negative-stained NPB in water showed a mixture of fibril structures,

[1]Departments of Biochemistry, University of Alberta, Edmonton, AB, Canada. [2]Departments of Oncology, University of Alberta, Edmonton, AB, Canada. [3]These authors contributed equally: John Maringa Githaka, Tomás Gutiérrez. ✉e-mail: ojulien@ualberta.ca; igoping@ualberta.ca

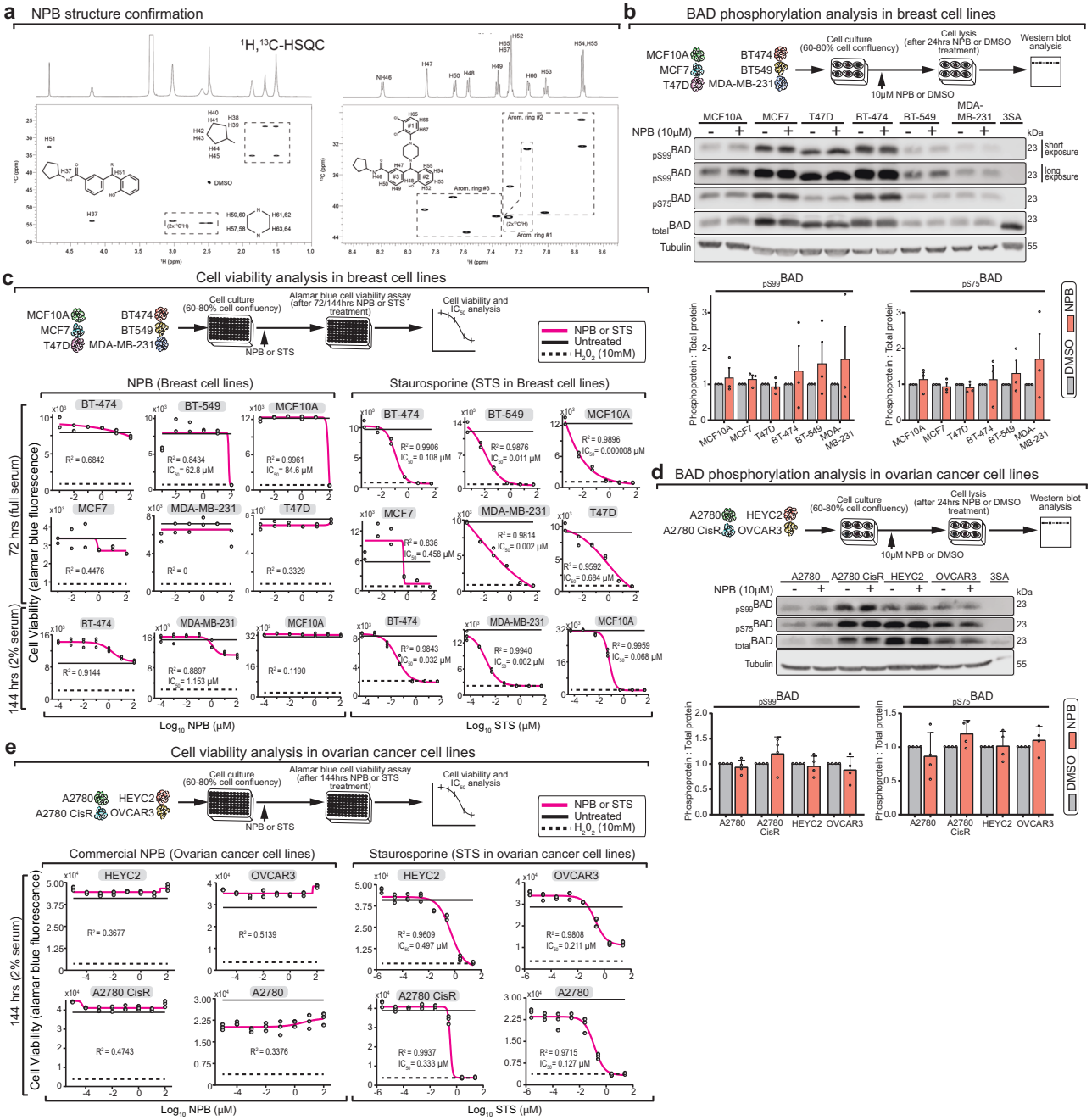

Fig. 1 | NPB structural confirmation, and minimal effect on BAD phosphorylation and cell viability. a NMR chemical shift assignment with 2D $^{1}H,^{13}C$-HSQC of commercial NPB shows aliphatic region featuring the ^{1}H-^{13}C bonds of the piperazine and cyclopentane rings (left) the three aromatic rings (right). **b** Western blots of breast cell lines treated with 10 μM NPB for 24 h. Control 3SA cell line[10] where serines 75, 99, and 118 are mutated to alanine shows specificity of phosphorylation antibodies. pBAD-Ser99 levels are shown with both short and long exposures. Data are mean ± SD of 3 biological replicates. **c** Alamar blue cell viability graphs of breast cells treated with increasing concentrations of NPB for 72 h or 144 h (left); and positive control staurosporine (STS) for 72 h or 144 h (right). Shown are representative data of 5 biological replicates for BT474, MCF10A and MDA-MB-231 with NPB for 72 h; 3 biological replicates for BT549, MCF7 and T47D with NPB 72 h; 1 biological replicate for NPB 144 h; 3 biological replicates for BT474, MCF10A and MDA-MB-231 with STS 72 h; 1 biological replicate for BT549, MCF7 and T47D with STS 72 h; and 1 biological replicate for STS 144 h. **d** Western blots of ovarian cell lines treated with 10 μM NPB for 24 h. Control 3SA cell line[10] where serine residues 75, 99, and 118 are mutated to alanine shows specificity of phosphorylation antibodies. Data are mean ± SD of 4 biological replicates (**e**) Alamar blue cell viability graphs of ovarian cells treated with increasing concentrations of NPB for 144 h (left); and positive control STS for 144 h (right). Shown are representative data of 3 biological replicates. The source data and statistical analysis are in the Supplementary Data file. Uncropped western blot images are provided in Supplementary Fig. 5.

colloids, and colloidal aggregates at 2 μM, 20 μM, and 100 μM (Fig. 2c). That NPB forms aggregates at the working concentrations reported to inhibit BAD phosphorylation and induce apoptosis[1,2] suggests that the published mechanism of cell death is likely not via binding to intracellular protein targets, such as BAD.

In summary, we could not confirm major findings on NPB cytotoxicity or mechanism of action while using the same cell lines, NPB source, NPB concentration ranges, and treatment parameters as the originating group[1,2]. We found that NPB was not cytotoxic to breast or ovarian cancer cell lines and had no effect on BAD phosphorylation. Importantly, we found that

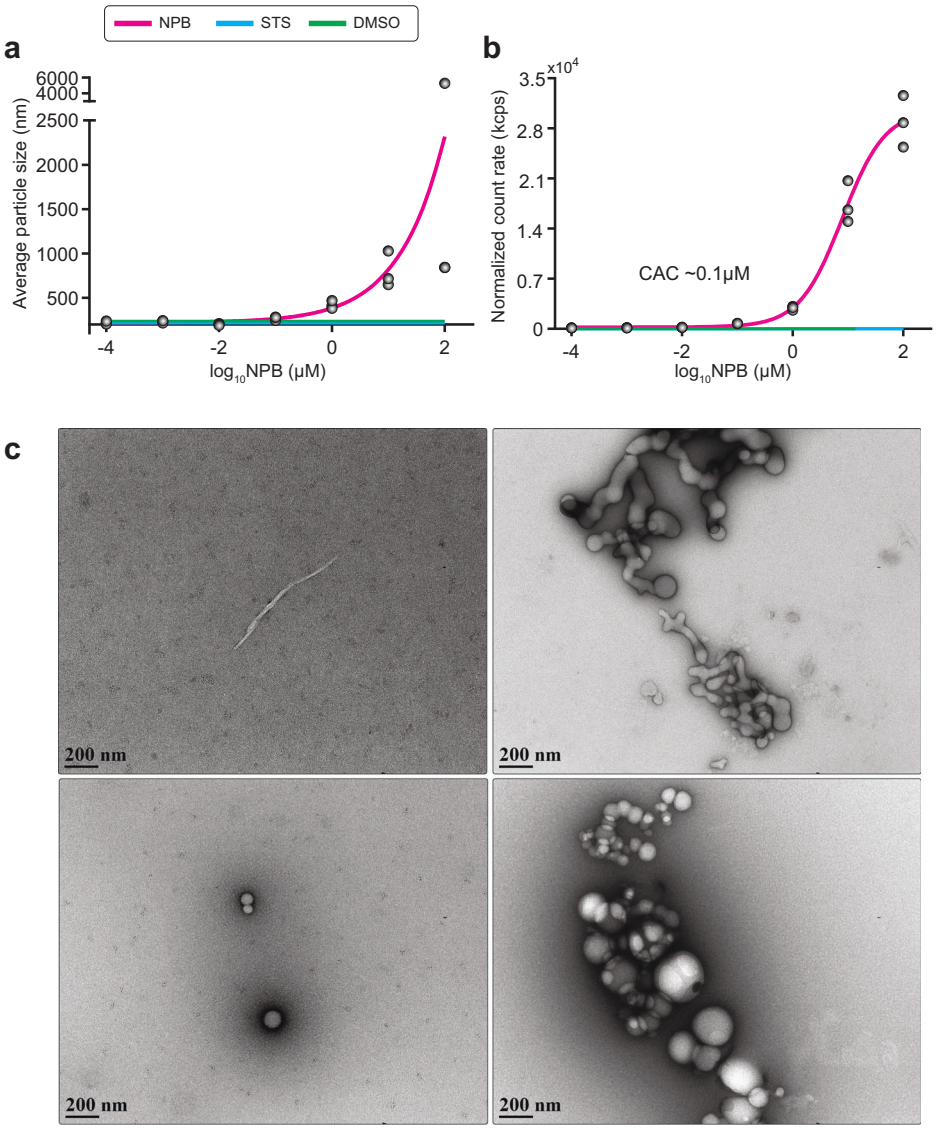

Fig. 2 | NPB forms concentration-dependent colloidal aggregates in aqueous. Dynamic Light Scattering showing (**a**) concentration dependent increase in measurement average particle size, and (**b**) normalized count rate relative to NPB concentration as a fitted non-linear regression curve to estimate critical aggregation concentration (CAC). **c** Representative electron micrographs of uranyl-acetate negative stained NPB at 2 μM and 20 μM (top row), and 100 μM (bottom row) concentrations, showing fibril, colloid, and aggregate colloid structures. STS is staurosporine; DMSO is dimethyl sulfoxide. The source data and statistical analysis are in the Supplementary Data file.

NPB forms colloidal aggregates at concentrations ~50-fold below the IC_{50}'s reported by the original group, and this has major implications for data interpretation. Small molecule forming colloidal or fibril aggregates may be inhibiting enzymatic activity in vitro[13], or can be toxic to cells[14]. Notably, small molecule aggregates constitute the majority of false-positive hits identified in drug screens[15]. Current recommendations are that small molecule discovery studies should always test for aggregation before reporting data (see work by the Shoichet lab[13,15,16]). That NPB forms colloidal aggregates in our hands, challenges the mechanism proposed by the originating group and suggests it is thus unlikely that NPB binds and inhibits intracellular BAD phosphorylation to activate the apoptotic program. We suggest these conflicting data along with the consequences of NPB aggregation should be fully considered before further investigations with NPB or analogous compounds are conducted.

Methods

NPB reconstitution

10 mg of NPB powder (from either Pandey et al. authors[2] or Axon Medchem cat# 3079, batch# 1) was diluted in 380 μL of DMSO (Sigma-Aldrich cat# 472301) for a stock concentration of 50 mM. The reconstituted NPB was stored in −20 °C, away from light. Two independent purchases of NPB were used in this study.

NPB structure validation

NMR spectra were acquired on a Varian INOVA 600 MHz spectrometer: 1D 1H, 2D 1H-1H-COSY, 1H,13 C HSQC and 1D 13 C observed using biopack pulse sequences. Data processing and analysis was performed using VnmrJ v4.2. The mass spectrometry data was acquired on a high-resolution Thermo Orbitrap XL using direct injection.

Cell culture

Six mammary cell lines (MCF10A, MCF7, T47D, BT-474, BT-549 and MDA-MB-231) were purchased in 2021, from ATCC with signed certificates of authentication. Cell lines routinely tested negative for mycoplasma contamination using Mycoplasma Pro PCR detection kit (Applied Biological Materials cat# G239). Similar to the Pandey et al. study[2], all breast cancer cell lines were cultured following ATCC recommendations. Specifically, (i) MCF7 in EMEM (ATCC cat# 30-2003) + 0.01 mg/ml human recombinant insulin (Gibco cat# 12585-014) + 10% FBS, (ii) T47D in RPMI-1640 + 0.2 Units/ml insulin (Sigma-Aldrich cat# I-1882) + 10% FBS, (iii) BT-474 in ATCC Hybri-Care Medium (ATCC cat# 46-X) + 10% FBS, (iv) BT-549 in RPMI-1640 (ATCC cat# 30-2001) + 0.023 U/ml insulin (Sigma-Aldrich cat# I-1882) + 10% FBS, and (v) MDA-MB-231 in Leibovitz's L-15 Medium (ATCC cat# 30-2008) + 10% FBS. Non-transformed mammary cell line MCF10A cells were cultured in DMEM/F12 (Gibco cat# 11330032) supplemented with 5% horse serum, 20 ng/mL EGF (Peprotech

cat# AF100-15), 0.5 µg/mL Hydrocortisone (Sigma-Aldrich cat# H-0888), 100 ng/mL Cholera toxin (Sigma-Aldrich cat# C-8052) and 10 µg/mL insulin (Sigma-Aldrich cat# I-1882). Four ovarian cancer cell lines were cultured following Zhang et al.[1] protocol: (i) A2780S in RPMI-1640 (Gibco cat# 22400105) + 10% FBS, (ii) A2780CisR in RPMI-1640 + 10% FBS + 1 µM cisplatin (Sigma-Aldrich cat# P4394), (iii) OVCAR3 in RPMI-1640 + 20% FBS + 10 µg/ml insulin (Sigma-Aldrich cat# I-1882) and (iv) HEYC 2 RPMI-1640 + 10% FBS. Both full and 2% FBS concentrations were tested in NPB treatment, and each case is specified in the figure legends.

Western blotting

300,000 cells per well were plated in 6 well plates and monitored until 60–80% cell confluency. Subsequently, fresh culture media with 10 µM NPB or equivalent DMSO volume was added for 24 h before cell scraping in lysis buffer (1% NP 40, 150 mM NaCl, 50 mM Tris-HCL pH 7.6, 5 mM EDTA, 1 mM EGTA, freshly added protease and phosphatase inhibitors). Soluble protein lysates were collected from the supernatant after a 20 min 14,000 × *g* centrifugation at 4 °C. Lysate concentration was determined by BCA assay and 20 µg of proteins were resolved on SDS-PAGE gels and transferred to nitrocellulose membranes. Primary antibodies used: rabbit-anti-BAD (Sigma-Aldrich cat# B0684), rabbit-anti-BAD-Ser99 (clone D25H8, Cell signaling cat# 4366), rabbit-anti-BAD-Ser75 (Cell signaling cat# 9291) and mouse-anti-Tubulin (clone B-5-1-2, Sigma-Aldrich cat# T5168). Secondary antibodies used: HRP and Alexa Flour 680 coupled anti-Rabbit and anti-mouse antibodies respectively. Blots were scanned using Odyssey LI-COR Fc imager (LI-COR Biosciences) in the chemiluminescence and 700 nm channels. Blot band intensities were quantified with Image Studio™ version 5.2 (LI-COR Biosciences), which applies a local background subtraction determined for each band. All BAD phosphorylation status was normalized to corresponding total BAD.

Alamar blue assay

Cells were plated in opaque 96-well plates with clear bottoms in the following concentrations: A2780S: 6000 cells/well, A2780CisR: 6000 cells/well, HEYC2: 6000 cells/well, OVCAR3: 12000 cells/well, BT-474: 15000 cells/well, BT-549: 2500 cells/well, MCF10A: 5000 cells/well, MCF7: 10000 cells/well, MDA-MB-231: 15000 cells/well and T47D: 15000 cells/well. Next day, cells were treated with NPB 0.0001, 0.001, 0.01, 0.1, 1, 10, 100, and 1000 µM. NPB was serially diluted in DMSO prior to dilution in media at final concentration. Control treatments included staurosporine 0.000005, 0.00005, 0.0005, 0.005, 0.05, 0.5, 5, and 50 µM. All assays included internal controls of cells treated with 10 mM H_2O_2 to indicate minimum cell viability, and vehicle (2% DMSO for breast cancer cell lines and 1% DMSO for ovarian cancer cell lines) to indicate maximum cell viability. After incubation time, media was discarded and replaced with fresh media with 10% alamar blue (In Vitro Toxicology Assay Kit, Resazurin based, Sigma-Aldrich, #TOX8) in a final volume of 100 µL per well. After 4 h, fluorescence was measured at excitation 560 nm, emission 590 nm in a microplate reader (Synergy, Bio-Tek). Representative graphs are shown. The 4 Parameter Logistic (4PL) regression model was used to fit the cell viability data. R-squared (goodness of fit) was computed to evaluate how well the experimental data could fit the 4PL model equation, with values ≥ 0.95 considered to be a good fit. Viability data plotting, 4PL fitting, R-squared and IC50 computations were done using GraphPad Prism7.

Reporting summary

Further information on research design is available in the Nature Portfolio Reporting Summary linked to this article.

Data availability

The source data and statistical analysis for Fig. 1b–e, Fig. 2a, b, Supplementary Fig. 3 and Supplementary Fig. 4b, c are in the Supplementary Data file. Uncropped western blot images are provided in Supplementary Fig. 5.

Received: 16 September 2022; Accepted: 24 April 2025;
Published online: 10 May 2025

References

1. Zhang, X. et al. Combined inhibition of BADSer99 phosphorylation and PARP ablates models of recurrent ovarian carcinoma. *Commun. Med.* **2**, 82 (2022).
2. Pandey, V. et al. Discovery of a small-molecule inhibitor of specific serine residue BAD phosphorylation. *Proc. Natl. Acad. Sci. USA* **115**, E10505–E10514 (2018).
3. Danial, N. N. BAD: undertaker by night, candyman by day. *Oncogene* **27**, 53 (2008).
4. Giménez-Cassina, A. & Danial, N. N. Regulation of mitochondrial nutrient and energy metabolism by BCL-2 family proteins. *Trends Endocrinol. Metab.* **26**, 165–175 (2015).
5. Zha, J., Harada, H., Yang, E., Jockel, J. & Korsmeyer, S. J. Serine phosphorylation of death agonist BAD in response to survival factor results in binding to 14-3-3 not BCL-X(L). *Cell* **87**, 619–628 (1996).
6. Yang, E. et al. Bad, a heterodimeric partner for Bcl-XL and Bcl-2, displaces Bax and promotes cell death. *Cell* **80**, 285–291 (1995).
7. Craik, A. C. et al. The BH3-only protein Bad confers breast cancer taxane sensitivity through a nonapoptotic mechanism. *Oncogene* **29**, 5381–5391 (2010).
8. Mann, J. et al. Non-canonical BAD activity regulates breast cancer cell and tumor growth via 14-3-3 binding and mitochondrial metabolism. *Oncogene* **38**, 3325–3339 (2019).
9. Mann, J. et al. BAD sensitizes breast cancer cells to docetaxel with increased mitotic arrest and necroptosis. *Sci. Rep.* **10**, 355 (2020).
10. Githaka, J. M. et al. BAD regulates mammary gland morphogenesis by 4E-BP1-mediated control of localized translation in mouse and human models. *Nat. Commun.* **12**, 2939 (2021).
11. Mabuchi, S. et al. Inhibition of phosphorylation of BAD and Raf-1 by Akt sensitizes human ovarian cancer cells to paclitaxel. *J. Biol. Chem.* **277**, 33490–33500 (2002).
12. Tafani, M., Minchenko, D. A., Serroni, A. & Farber, J. L. Induction of the mitochondrial permeability transition mediates the killing of HeLa cells by Staurosporine1. *Cancer Res.* **61**, 2459–2466 (2001).
13. Irwin, J. J. et al. An aggregation advisor for ligand discovery. *J. Med. Chem.* **58**, 7076–7087 (2015).
14. Julien, O. et al. Unraveling the mechanism of cell death induced by chemical fibrils. *Nat. Chem. Biol.* **10**, 969–976 (2014).
15. McGovern, S. L., Caselli, E., Grigorieff, N. & Shoichet, B. K. A common mechanism underlying promiscuous inhibitors from virtual and high-throughput screening. *J. Med. Chem.* **45**, 1712–1722 (2002).
16. Ganesh, A. N., Donders, E. N., Shoichet, B. K. & Shoichet, M. S. Colloidal aggregation: from screening nuisance to formulation nuance. *Nano Today* **19**, 188–200 (2018).

Acknowledgements

We are grateful to all Goping lab members for their valuable discussions and contribution. We thank Rakesh Bhat for advice on DLS measurements. This work was supported by an operating grant from Canadian Institutes of Health Research, Canadian Cancer Institute, and Lilian McCullough endowed Chair to ISG, Canadian Institutes of Health Research to HSY, and Canada Foundation for Innovation.

Author contributions

I.S.G. and J.M.G. conceptualized the study. J.M.G., T.G., Z.Z.H., J.O.P., H.M., B.D.S., and O.J. performed the experiments. J.M.G., T.G., J.O.P., B.D.S., and O.J. analyzed the data. B.D.S., H.S.Y., O.J., and I.S.G. supervised the study. I.S.G. directed research. J.M.G. and I.S.G. wrote the paper. J.M.G. and T.G. contributed equally to the study. O.J. and I.S.G. co-supervised equally to the study.

Competing interests
The authors declare no competing interests.

Additional information
Supplementary information The online version contains supplementary material available at https://doi.org/10.1038/s43856-025-00880-0.

Correspondence and requests for materials should be addressed to Olivier Julien or Ing Swie Goping.